

Preparation of PEG Reinforced Bamboo Cellulose Acetate Membrane Materials and Its Properties

Ekiñe Celada ¹, Richard Driller ², Marc Tiso ^{2,*}

¹ Flemish Institute for Technological Research (VITO N.V.), Boeretang 200, Mol, 2400, Belgium

² Institute of Systems Biotechnology, Saarland University, Campus A1.5, D-66123 Saarbrücken, Germany

*Corresponding author: Marc.tiso@uni-saarland.de

Abstract. In this paper, cellulose was extracted from *Dendrocalamus sinicus*, a giant bamboo species specially distributed in southwest China. Bamboo cellulose acetate (BCA) was prepared by using acetic anhydride as acetyl agent and concentrated sulfuric acid as catalyst. Then the polyethylene glycol (PEG 200), a kind of non-toxic and non-irritating plasticizer, was used as additive to prepare cellulose acetate/polyethylene glycol composite membrane material. The properties of the polyethylene glycol reinforced membrane materials were studied by the methods of SEM, IR, tensile properties and contact angle. The results showed that the purity of the bamboo cellulose was 93.46%, the cellulose acetate acetyl content was 48.54%, and the degree of substitution was 1.99. PEG was successfully loaded on the cellulose acetate/polyethylene glycol composite membrane, the structure of cellulose acetate itself was not changed, and the inner structure of the composite membrane was more compact. The tensile strength and fracture elongation increased by 13.42% and 114.76% respectively. The UV barrier effect was better than that of the base membrane, the contact angle reduced from 93 to 28, and the hydrophilicity greatly increased. The thermal stability of the material was slightly reduced after the addition of PEG.

Keywords: *Dendrocalamus sinicus*; Cellulose acetate; Polyethylene glycol; Membrane; Characterization

Received on 15 Sep 2024, Accepted on 15 Oct 2024, Published on 15 Dec 2024

Copyright © 2024 Ekiñe Celada *et al.* licensed to JGEEEE. This is an open access article distributed under the terms of the CC BY-NC-SA 4.0, which permits copying, redistributing, remixing, transformation, and building upon the material in any medium so long as the original work is properly cited.

1 Introduction

Since the 21st century, the energy crisis and resource depletion caused by world population growth have become increasingly serious, thus the development and utilization of continuously renewable cellulose fibers have received widespread attention [1]. Due to problems such as competition for land with food crops and impact on arable land area in large-scale production of traditional natural cellulose fiber raw materials such as cotton, ramie, wood, etc., people have increasingly focused on the development of new natural, sustainably utilizable cellulose fibers [2]. China has abundant bamboo resources. Bamboo is a fast-growing plant with high yield, numerous varieties, wide uses, and its strength, toughness, hardness and other properties are significantly better than wood [3]. Bamboo fiber can completely degrade in soil, causing no strong damage to the natural environment, known as an environmentally friendly fiber raw material. In industrial production, membrane materials made from cellulose derivatives have long been used [4]. Especially in recent years, as countries pay more attention to environmental protection and sustainable resource utilization, various emerging environmentally friendly membrane materials emerge in an endless stream with numerous types, and cellulose membrane materials are one of the important topics.

Cellulose acetate (CA), a representative thermoplastic cellulose derivative synthesized via the acetylation of hydroxyl groups on cellulose chains extracted from lignocellulosic biomass, has emerged as one of the most extensively utilized biopolymers in modern materials science and industrial engineering owing to its exceptional biodegradability, biocompatibility, mechanical processability, optical transparency, chemical stability, and

structural tunability [5]. As a renewable and eco-friendly alternative to conventional petroleum-based polymers, CA has been widely investigated and applied in diverse advanced fields, including membrane separation, biomedical engineering, environmental remediation, optical devices, textile manufacturing, packaging materials, and energy storage systems, demonstrating remarkable adaptability to multifunctional material design. In membrane-based separation technologies, cellulose acetate and its modified derivatives dominate the fabrication of microfiltration, ultrafiltration, nanofiltration, and reverse osmosis membranes, which are extensively employed for seawater desalination, brackish water purification, industrial wastewater treatment, removal of heavy metal ions, organic contaminants, dyes, pharmaceuticals, and pathogenic microorganisms, owing to their favorable hydrophilicity, controllable porosity, low fouling tendency, and cost-effective fabrication; moreover, CA-based membranes exhibit promising performance in gas separation applications, such as carbon dioxide capture, hydrogen purification, oxygen/nitrogen selectivity, and natural gas upgrading, attributed to their high gas solubility, appropriate chain mobility, and resistance to aggressive chemical environments. In biomedical and pharmaceutical sectors, the non-toxic, non-irritating, and bioinert nature of cellulose acetate enables its broad utilization in controlled drug delivery systems, including microspheres, nanoparticles, hydrogels, implants, and transdermal patches, where drug release kinetics can be precisely modulated by tailoring the degree of substitution, crosslinking density, pore structure, and surface chemistry of the CA matrix; additionally, CA is widely applied in tissue engineering scaffolds, wound dressings, surgical sutures, hemodialysis membranes, biosensor substrates, and diagnostic devices, providing reliable interfaces for biological tissues and fluids while supporting cell adhesion, proliferation, and differentiation. As an important fibrous material, cellulose acetate fibers and tows are globally used in cigarette filtration systems due to their high adsorption capacity for harmful components, uniform morphology, and biodegradability, whereas CA textile fibers are favored in apparel, home textiles, and decorative fabrics for their soft texture, excellent drapability, luster, breathability, wrinkle resistance, and dyeability. In optical and electronic applications, cellulose triacetate (CTA), a high-substitution derivative of CA, serves as a critical substrate for liquid crystal display polarizers, photographic films, X-ray films, and protective optical coatings, owing to its outstanding optical clarity, dimensional stability, and mechanical durability; meanwhile, CA-based composites are increasingly integrated into flexible electronic devices, insulating materials, and protective coatings, expanding their utility in modern electronic manufacturing. In environmental and packaging fields, cellulose acetate films and composites represent promising biodegradable packaging materials for food, cosmetics, and industrial products, providing balanced barrier properties against moisture, oxygen, and volatile organic compounds while alleviating the environmental burden caused by non-degradable plastics; furthermore, surface-modified and hydrophobic CA materials have demonstrated superior efficiency in oil-water separation, membrane distillation, and pollutant adsorption, contributing significantly to environmental governance and resource recovery. In energy-related applications, CA acts as an ideal separator material for lithium-ion batteries and supercapacitors, offering high ionic conductivity, robust mechanical strength, and electrochemical stability to enhance device safety and cycling performance; it also functions as a binder, coating agent, and structural modifier in composite materials, improving processability, adhesion, and functional durability. With continuous advances in green synthesis, nanocomposite incorporation, surface functionalization, 3D printing, and recycling technologies, the performance and application scope of cellulose acetate are being further expanded, enabling its integration into emerging fields such as smart responsive materials, biosensing platforms, biodegradable actuators, water harvesting systems, and advanced biomedical devices. As a sustainable and versatile biopolymer, cellulose acetate not only bridges the gap between biomass resources and high-performance functional materials but also addresses global challenges related to plastic pollution, energy shortage, and environmental degradation, solidifying its irreplaceable role in both fundamental scientific research and practical industrial applications for a low-carbon and circular economy.

Due to the coexistence of non-crystalline regions and complex crystalline regions in the macroscopic morphological structure of cellulose, and strong intermolecular forces at the microscopic level, a large number of hydroxyl groups on cellulose molecular chains form hydrogen bonds [6]. Therefore, in the preparation process of cellulose membrane materials, cellulose generally needs to be chemically modified before it can be utilized. To reduce the polarity of cellulose and enhance its mechanical properties, hydrophilicity, flame retardancy, and stability, scholars have conducted various modification studies on cellulose, such as acetylation, hydroxypropylation, sulfonation, etc. Cellulose acetate is prepared by the reaction of cellulose with acetylating agent acetic anhydride [7]. Additionally, it is usually necessary to add some modifying materials to improve and enhance the properties of cellulose materials, so that the material obtains the properties endowed by the modifying material while its own material properties remain unchanged or change slightly [8]. This study uses

polyethylene glycol as an additive to adjust the polymer state in the casting solution thereby improving the membrane's structural morphology to enhance various aspects of the membrane's performance. Polyethylene glycol has good water solubility, is non-toxic and harmless, has strong moisturizing properties, good dispersibility, and can dissolve with many organic components, being widely used in the modification of polymer membrane materials [9]. Yin Cheng added different amounts of titanium dioxide on the basis of polyethylene glycol improving membrane performance to investigate the effect of titanium dioxide on membrane hydrophobicity and antifouling properties [10]; KH Kim used polyethersulfone composite hollow fiber membrane to separate water vapor from mixed gases, coated with cellulose acetate [CA] and polyethylene glycol [PEG] to improve the separation performance of the membrane [11]. Due to the good water solubility of PEG, the permeability and selectivity of the membrane increased with the increase of PEG content and molecular weight in the coating solution; Kibrom modified the microstructure of cellulose acetate ultrafiltration membrane by adding polyethylene glycol, improving the permeability and antifouling properties of the membrane; Ahmad prepared a series of cellulose acetate/polyethylene glycol membranes with different ratios through a two-stage inversion scheme, and after optimizing different ratios, prepared a membrane material with the highest desalination capability. It can be seen that polyethylene glycol [12], as a non-toxic, harmless, and inexpensive hydrophilic additive, has been widely studied in improving material properties with good results, but there is no specific report on the improvement of *Dendrocalamus sinicus* cellulose membrane properties by polyethylene glycol [13].

This study uses *Dendrocalamus sinicus*, a large characteristic bamboo species from southwest China, as raw material to prepare cellulose acetate base membrane, then selects polyethylene glycol as modifier to prepare cellulose acetate polyethylene glycol composite membrane. The properties of the base membrane and composite membrane are characterized and compared through scanning electron microscopy, contact angle measurement, tensile property measurement, and infrared spectroscopy and other analytical detection methods. The effects of polyethylene glycol on the film formation effect, mechanical properties, light transmission properties, and hydrophilicity/hydrophobicity of *Dendrocalamus sinicus* cellulose membrane materials are investigated, to provide a theoretical basis for the further modification and optimization of membrane materials and the comprehensive development and utilization of *Dendrocalamus sinicus*.

2 Materials and Methods

2.1 Preparation of *Dendrocalamus sinicus* Cellulose

Dendrocalamus sinicus bamboo wood was air-dried, crushed, sieved, mixed, quartered, and powder samples with particle size of 0.25~0.42 mm were screened out. The bamboo powder was extracted with toluene:ethanol [2:1, v/v] solution for 10 h to remove wax, dried at 60°C, then delignified with NaClO₂ [2]. Bamboo powder and NaClO₂ powder were added to a three-necked flask at a ratio of 1:1 [w/w], then distilled water was added, solid:liquid = 1:10 [w/v], pH adjusted to 3.8~4 with 6 mol·L⁻¹ HCl, refluxed for 1 h in a 75°C water bath. NaClO₂ powder equivalent to 0.5 times the mass of bamboo powder was added, pH adjusted to 3.8~4, refluxed again in a 75°C water bath for 1 h, then filtered, the filter residue washed with water to pH=7, dried at 75°C to obtain holocellulose. 10% NaOH solution was added, solid-liquid ratio 1:20 [w/v], stirred at room temperature for 16 h, filtered, the filter residue washed to neutrality, dried to obtain the desired *Dendrocalamus sinicus* cellulose.

2.2 Preparation of *Dendrocalamus sinicus* Cellulose Acetate

In brief, 5 g of *Dendrocalamus sinicus* cellulose powder was placed in a flask, 50 mL of glacial acetic acid added, soaked in a 50°C water bath for 3 h. Then 40 mL of acetylating agent acetic anhydride and 250 μL of concentrated sulfuric acid as catalyst were added, stirred in a 50°C water bath for 2.5 h. After the reaction, centrifuged, the supernatant was poured into distilled water to precipitate loose white flocculent precipitate. Filtered, the filter residue washed to neutrality, freeze-dried to obtain *Dendrocalamus sinicus* cellulose acetate [BCA] sample.

2.3 Preparation of Cellulose Acetate Membrane Materials

First, the BCA sample was placed in a 60°C blast drying oven for 10 h, the material layer thickness controlled below 3 cm, while PEG was heated to 60°C for activation, then 40 wt% PEG was added to BCA, stirred manually for 20~30 min to allow the plasticizer and raw material to fully mix. The mixture was sealed and placed in a 60°C

blast drying oven for 10 h to allow BCA to fully absorb the plasticizer, obtaining

0.6 g of BCA sample and BCA-PEG sample were each placed in a beaker, 20 mL of trichloromethane added to each, stirred in a 40°C water bath for 2.5 h. After fully dissolved, the clear solution was poured into a prepared dry mold, placed in a fume hood to air-dry for 10 h. After the solvent completely evaporated, the membrane was peeled off from the mold, the surface wiped with cotton dipped in a small amount of distilled water to remove possible dust, finally wiped dry with filter paper to obtain the cellulose acetate base membrane [BCA membrane] and cellulose acetate-polyethylene glycol composite membrane [BCA-PEG membrane]. The prepared samples were stored in a desiccator for analysis.

2.4 Characterization of Membrane Materials

2.4.1 Determination of *Dendrocalamus sinicus* Cellulose Component Content

The three major components content was determined referring to the American National Renewable Energy Laboratory [NREL] standard. Lignin content $w = w_{\text{acid-insoluble lignin}} + w_{\text{acid-soluble lignin}}$, cellulose and hemicellulose content determined by high performance liquid chromatography. The chromatographic column was Japanese CAPCELLPAK C18 column [5 μm , 4.6 mm \times 250 mm], column temperature 30°C, using acetonitrile: potassium dihydrogen phosphate [0.05 mol·L⁻¹] with volume ratio 25:75 as mobile phase, flow rate 1.0 mL·min⁻¹, injection volume 10 μL .

2.4.2 Determination of Acetyl Group Content in Cellulose Acetate

By measuring the acetyl group content in the sample, the degree of substitution of active hydroxyl groups in the cellulose raw material was analyzed. The method referred to the "Pharmacopoeia of the People's Republic of China" [14], to determine the acetyl group content of the cellulose acetate membrane raw material. The degree of substitution [DS] of cellulose acetate was calculated using the acetyl group content, the relationship between acetyl group content and degree of substitution is as follows:

$$\text{Acetyl group content [\%]} = [60 \times d \times 100] / [162 + 42 \times d]$$

Where d is the degree of substitution; 162 is the molecular weight per glucose unit; 60 is the molecular weight of acetic acid; 42 is the increase after acetyl group substitution for hydrogen.

2.4.3 Scanning Electron Microscopy Analysis Method

The microstructure of the membrane samples was examined by SEM to analyze the morphological characteristics of the sample surface and cross-section. Before testing, the membrane samples were placed in liquid nitrogen, brittle fractured using clean tweezers in liquid nitrogen, then the cross-section was observed. The sample surface needed to be sputter-coated with gold before testing to avoid electron beam interference from charges on the sample surface. During testing, the acceleration voltage was about 15 kV, magnification 2000~20000.

2.4.4 Infrared Spectroscopy Analysis Method

The potassium bromide pellet method was used. The sample was ground and uniformly dispersed in potassium bromide powder, sample concentration about 1 wt%. Scanned in the wavenumber range 4000~400 cm^{-1} , number of scans 32, resolution 4 cm^{-1} .

2.4.5 Tensile Property Determination Method

The maximum tensile force and maximum deformation that the membrane sample could withstand were measured to calculate the tensile strength and elongation at break of the membrane sample. The experiment was conducted at room temperature, the test membrane sample size was 5 cm \times 2.5 cm, tensile speed 5 mm·min⁻¹. Tensile strength and elongation at break were calculated according to the following formulas:

$$\text{Tensile strength } \delta \text{ [MPa]} = F / [b \times d] \text{ [1]}$$

In formula [1], F is the maximum tensile force the sample can withstand N; b is the sample width mm; d is the

sample thickness mm.

Elongation at break ϵ [%] = $[\Delta L / L_0] \times 100\%$ [2]

In formula [2], ΔL is the maximum deformation the membrane sample can withstand mm; L_0 is the initial distance between the test fixtures mm.

2.4.6 UV-Vis Transmittance Analysis Method

The change of transmittance of the membrane sample with light wavelength was analyzed to detect the light transmission performance of the sample. The wavelength variation range was 200~800 nm.

2.4.7 Contact Angle Measurement Method

The hydrophobic performance of the sample was analyzed by measuring the angle between the water droplet and the sample on the membrane sample. Each sample was measured three times repeatedly, and the average value was calculated.

2.4.8 Thermal Stability Analysis Method

The stability of the sample at high temperature was detected by analyzing the relationship between the sample mass and the temperature rise during uniform heating. Before testing, the sample was dried in an oven at 70°C for 2 h, then 5~10 mg of sample was taken for analysis. Heating rate 10°C·min⁻¹, nitrogen flow rate 30 mL·min⁻¹, test temperature from 25°C heated to 800°C.

3 Results and Discussion

3.1 Analysis of Dendrocalamus sinicus Cellulose Component Content

To analyze the composition of the membrane raw material, the cellulose obtained from the component separation of *Dendrocalamus sinicus* was tested for composition. The data results showed that the raw material contained 3.07% hemicellulose, 93.46% cellulose, and 3.31% lignin.

3.2 Analysis of Cellulose Acetate Acetyl Group Content

To characterize the acetylation degree of the prepared *Dendrocalamus sinicus* cellulose acetate, the acetyl group content of the cellulose acetate was detected, and its degree of substitution was calculated using the formula. The acetyl group content of *Dendrocalamus sinicus* cellulose acetate [BCA] was measured to be 48.54%, and the degree of substitution was 1.99.

3.3 Infrared Spectroscopy Analysis

Figure 1 shows the infrared spectra of the BCA-PEG composite membrane and the BCA membrane. It can be seen from the figure that the infrared spectra of the BCA-PEG composite membrane and the BCA membrane have high similarity. The infrared characteristic peaks were assigned with reference to related literature [17-18]. Compared with the BCA membrane, the stretching vibration peaks near 3441 cm⁻¹ and 2873 cm⁻¹ in the infrared spectrum of the BCA-PEG composite membrane are enhanced due to the hydroxyl and methylene groups in PEG. The similarity is manifested in the sharp absorption peak at 1740 cm⁻¹ caused by C=O in the acetyl group; the bending vibration peak of -CH₃ at 1367 cm⁻¹; the stretching vibration peaks of C-O-C in cellulose acetate at 1212 cm⁻¹ and 1035 cm⁻¹; the absorption peak of β -glycosidic bond at 896 cm⁻¹. The infrared spectroscopy proves that PEG is successfully loaded and does not change the structure of cellulose acetate itself.

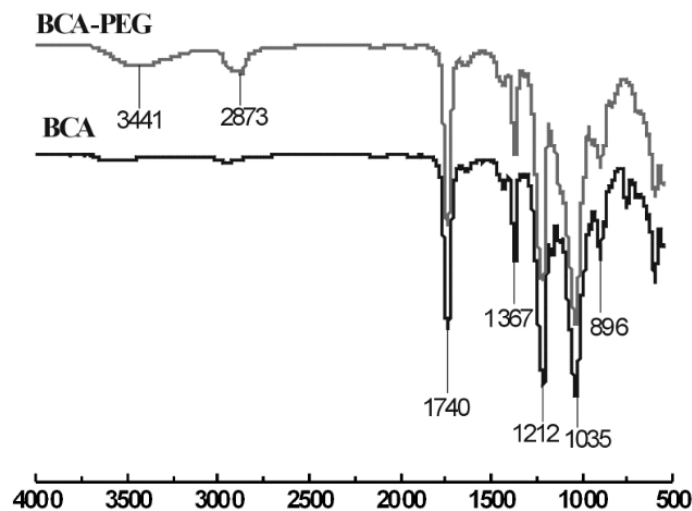


Figure 1 FT-IR spectra of the cellulose acetate film BCA-PEG and BCA

3.4 Scanning Electron Microscopy Analysis

Figure 2 shows the scanning electron microscopy [SEM] images of the membrane materials. The experiment used the solvent evaporation phase separation method with mild conditions to prepare the membrane materials. a and b are the surface and cross-section images of the BCA-PEG composite membrane, respectively; c and d are the surface and cross-section images of the BCA base membrane, respectively; e and f are the surface and cross-section images of cellulose acetate membrane prepared by non-solvent induced phase separation method [referred to as NIPS membrane] from related literature [19], used for comparison. Since they are quoted from literature for comparison, the magnification is different, and the data are for reference analysis only. The principles of the solvent evaporation phase separation method and the non-solvent induced phase separation method for membrane preparation are the same, both separate the solvent of cellulose acetate from the system. The difference is that the solvent evaporation phase separation method uses the high volatility of the selected solvent to diffuse the solvent into the air. This process is relatively slow, mild, and uniform. The non-solvent induced phase separation method diffuses the solvent into another solvent in which cellulose acetate is insoluble. This process is relatively fast and intense, which may easily affect the structure of the resulting cellulose acetate membrane.

From the micromorphology images, it can be seen that the surfaces of all three membranes are relatively flat without obvious defects such as pinholes or cracks. There are some impurities adsorbed on the surface of the base membrane in figure c, while the surface of the composite membrane in figure a has few impurities, which may be due to the improved antifouling performance of the membrane material after adding PEG [20].

The cross-sections of the composite membrane and the base membrane show no obvious pores or cracks, while the cross-section of the NIPS membrane in figure f contains many irregular pores, indicating that the solvent evaporation phase separation method used in this study produces a flatter and denser membrane structure compared to the non-solvent induced phase separation method. The cross-section of the BCA-PEG composite membrane is flatter and the structure is denser than that of the BCA base membrane. Clearly, the addition of PEG makes the internal structure of the cellulose acetate membrane tighter.

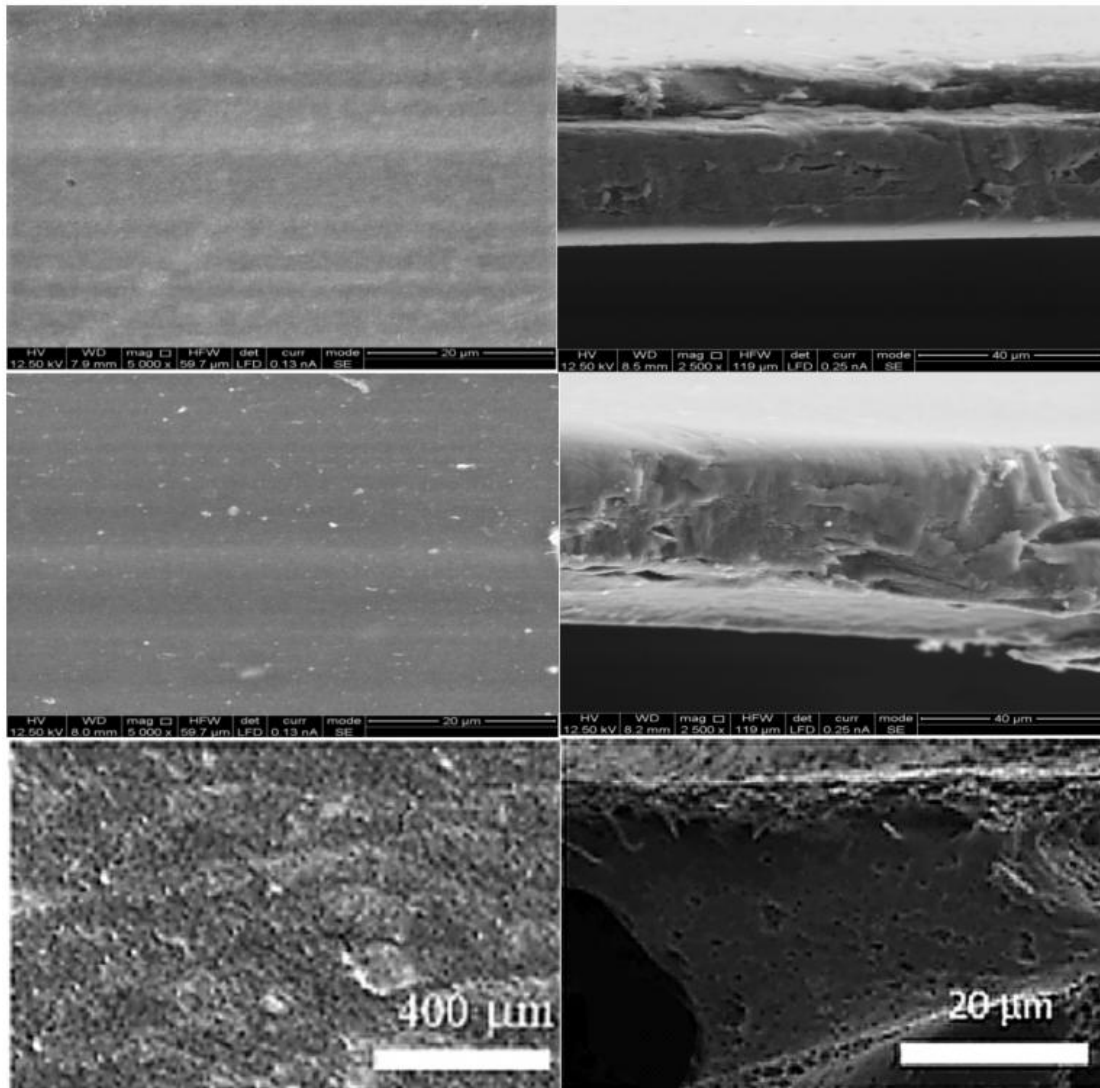


Figure 2 SEM images of membrane material

3.5 Tensile Performance Analysis

The tensile strength and elongation at break of the BCA-PEG composite membrane were measured, and the results were compared with the BCA base membrane data, as shown in Figure 3. It can be seen from the figure that the tensile strength of the BCA-PEG composite membrane is 52.14 MPa, which is 13.42% higher than that of the base membrane. The elongation at break is 4.51%, which is 114.76% higher than that of the BCA base membrane. Clearly, the addition of PEG enhances the mechanical properties, especially the toughness, of the cellulose acetate membrane material. PEG is not only non-toxic and harmless and low-cost, but also highly effective in improving the mechanical properties of the membrane. According to the research results of Wang Xia [21] on the effects of different types of plasticizers on the mechanical properties of membrane materials, the tensile strength is closely related to the number of hydroxyl groups on the structural unit of PEG. PEG has long molecular chains and a large number of hydroxyl groups, resulting in strong interaction with cellulose molecules. Therefore, the strength of the membrane material prepared after adding PEG is greater than that of membrane materials prepared with other types of plasticizers. Moreover, the plasticizer PEG-200 added in the experiment is a small molecule substance. The addition of small molecule substances reduces the intermolecular forces of the membrane material, significantly enhancing the elongation at break of the membrane material. The interface between polyethylene glycol and cellulose acetate transfers the external force borne by the composite material system to polyethylene glycol, preventing crack propagation and slowing stress concentration [22-23], improving the mechanical properties of the material and expanding its application fields.

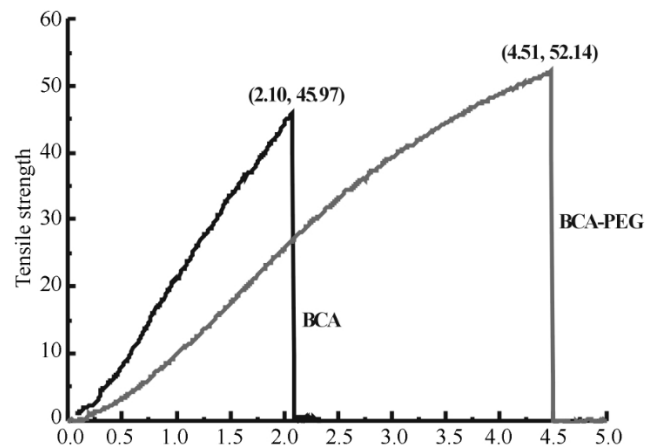


Figure 3 Tensile property of the cellulose acetate film BCA-PEG and BCA

3.6 UV-Vis Light Transmittance Analysis

Figure 4 shows the change images of the transmittance of the BCA-PEG membrane and the BCA membrane in the wavelength range of 200~800 nm. In the electromagnetic spectrum, the ultraviolet region is 10~400 nm, and the visible light region is 400~760 nm [24]. It can be seen from the figure that the transmittance of both the BCA-PEG membrane and the BCA membrane in the visible light region is around 90%. In the ultraviolet region, the transmittance of the BCA-PEG composite membrane is generally lower than that of the BCA base membrane, except in the short-wave ultraviolet region of 200~250 nm, where the transmittance of the BCA-PEG composite membrane is higher. In summary, the BCA-PEG composite membrane has a stronger blocking effect on ultraviolet light than the BCA base membrane.

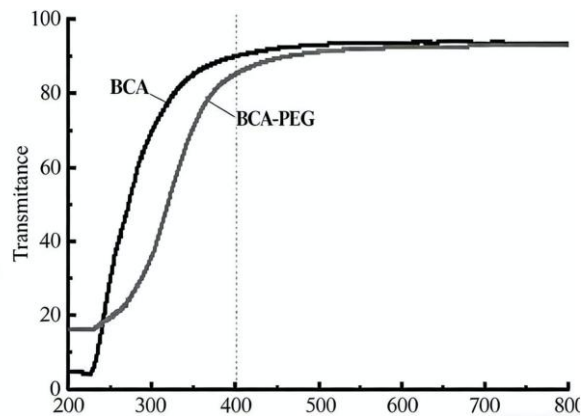


Figure 4 UV-Vis spectra of the cellulose acetate film BCA-PEG and BCA

3.7 Contact Angle Measurement

This study compared the hydrophilicity of the BCA-PEG composite membrane and the BCA base membrane by detecting the spreading ability of water droplets on the membrane material surface [25-26]. Scholar Wang Dongsheng [27] conducted a detailed study on the hydrophilic modification of cellulose membranes by adding PEG alone. He found that as the amount of PEG increased, the contact angle continuously decreased and the hydrophilicity improved. When the PEG concentration was small, below 4 wt%, the contact angle did not change significantly. When the concentration was greater than 4 wt%, the contact angle decreased markedly. Furthermore, Wang Dongsheng reduced the contact angle of the cellulose membrane to 30° by adding PEG-400, preparing a membrane material with good hydrophilicity. In this study, to further improve the material properties, 40 wt% PEG-200 was added to the composite membrane. The obtained hydrophilicity improvement results are shown in Figure 5. It can be seen from the figure that the average contact angle of the BCA-PEG composite

membrane reached 28.2°, while the average contact angle of the BCA base membrane was 93°. The hydrophilicity of the BCA-PEG composite membrane was 69.6% stronger than that of the BCA base membrane. The main reason for such a large increase in hydrophilicity is that the modifier PEG has relatively strong hydrophilicity. Therefore, it is evident that PEG is a very suitable hydrophilic modifier.

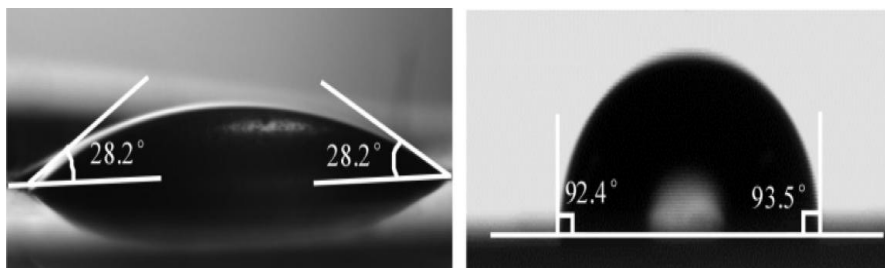


Figure 5 Droplet images on the surface of the cellulose acetate film (a) BCA-PEG and (b) BCA

3.8 Thermal Stability Analysis

Figure 6 shows the TG/DTG curves of the BCA-PEG composite membrane and the BCA base membrane. From the start of the test to the 150°C stage, the weight loss of both the BCA-PEG composite membrane and the BCA base membrane was not significant. The weight loss in this stage was mainly caused by the evaporation of water in the membrane sample. The BCA-PEG composite membrane began to enter the first rapid weight loss stage from 150°C and reached the maximum weight loss rate at 215°C. The weight loss slowed down around 300°C. This stage is the decomposition and weight loss stage of the PEG in the composite membrane. The weight loss in this stage was close to 40%, which is close to the mass fraction of PEG added to the cellulose acetate. Starting from 300°C, both the composite membrane and the base membrane entered the main pyrolysis stage together. This stage is mainly the pyrolysis of cellulose acetate. The BCA-PEG composite membrane and the BCA base membrane reached their maximum pyrolysis rates at 348.3°C and 358.3°C, respectively, and the weight loss slowed down for both around 420°C. The above analysis results indicate that the addition of PEG slightly reduces the thermal stability of the composite membrane.

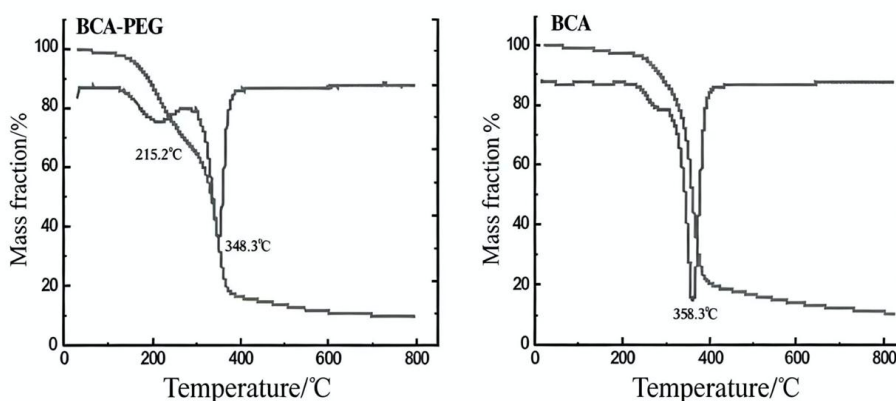


Figure 6 TG and DTG curves of the cellulose acetate film BCA-PEG and BCA

3.9 Underlying mechanisms for enhanced properties

Based on the comprehensive experimental data and characterization results presented in the document, the mechanism underpinning the performance enhancement of the polyethylene glycol (PEG)-reinforced bamboo cellulose acetate (BCA) composite membrane is fundamentally attributed to the effective plasticization and microstructural modification of the cellulose acetate matrix by the PEG molecules, which operates through physical intermolecular interactions rather than chemical alteration. The process initiates during the film preparation, where activated PEG (PEG-200) is thoroughly mixed with BCA at a 40 wt% loading and allowed to be absorbed into the polymer matrix. Upon dissolution in chloroform and subsequent solvent evaporation, the

core mechanism involves the intercalation of the low-molecular-weight, linear PEG chains within the amorphous regions of the cellulose acetate polymer chains. The PEG molecules, possessing a high density of ether oxygen atoms (-O-) and terminal hydroxyl groups (-OH), act as a molecular spacer. They form extensive hydrogen bonds and dipole-dipole interactions with the carbonyl (C=O) and remaining hydroxyl groups on the cellulose acetate backbone, as suggested by the enhanced infrared absorption peaks at 3441 cm^{-1} (O-H) and 2873 cm^{-1} (C-H) in the BCA-PEG composite spectrum compared to the pure BCA film. This intermolecular interaction is crucial as it disrupts the native hydrogen-bonding network and reduces the cohesive forces between the cellulose acetate chains, thereby increasing the free volume and chain mobility within the polymer matrix. This plasticizing effect directly explains the dramatic 114.76% increase in elongation at break, as the more mobile chains can undergo greater deformation before fracture. Concurrently, the significant 13.42% improvement in tensile strength is mechanistically linked to the stress-transfer capability of the well-dispersed PEG phase; the strong interfacial adhesion via hydrogen bonding allows external stress applied to the composite to be efficiently transferred and dissipated throughout the PEG/BCA interface, preventing crack initiation and propagation, which aligns with the referenced literature on interface behavior. The formation of a denser and more compact internal microstructure, as unequivocally observed in the SEM cross-sectional images of the BCA-PEG film compared to the more heterogeneous BCA base film, is another direct consequence of this plasticization. The PEG molecules fill the interstitial spaces and micro-voids that might form during the solvent evaporation process, leading to a more homogeneous and less defective morphology.

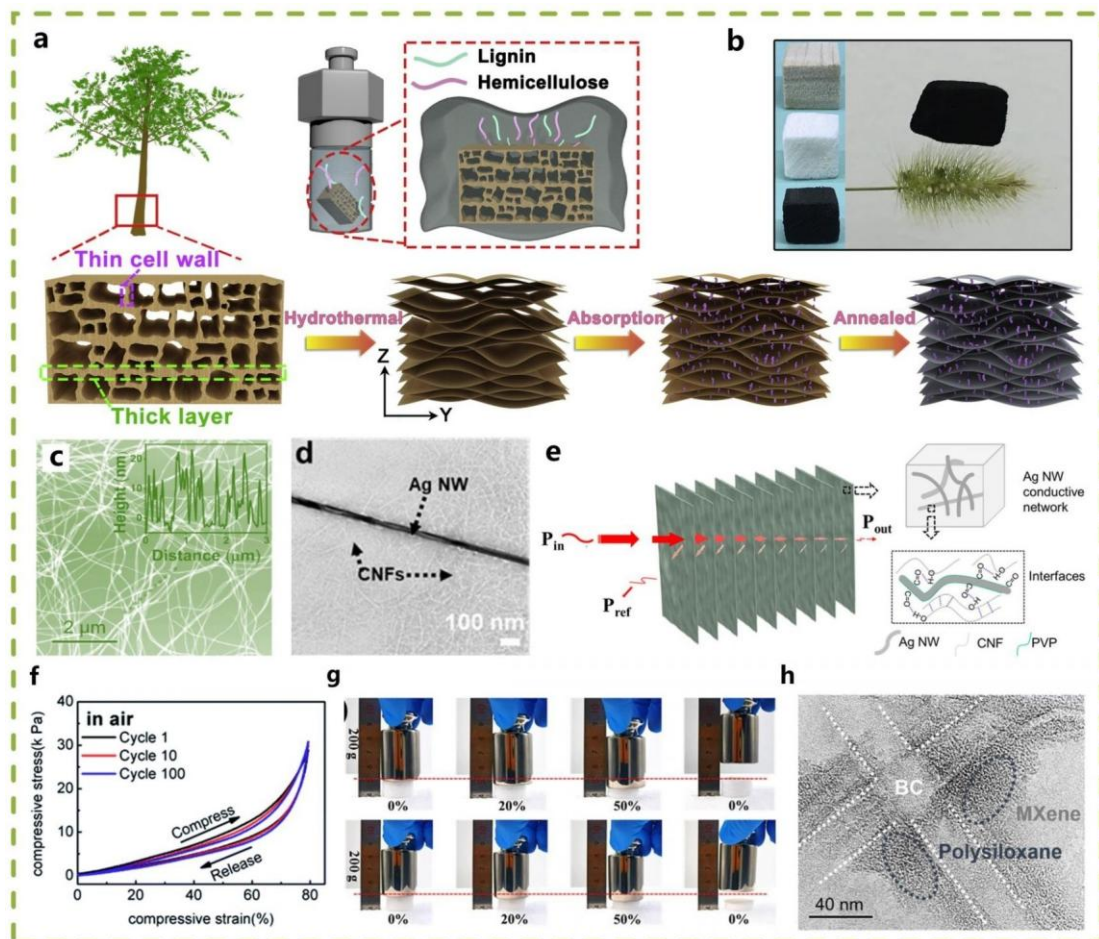


Figure 7 Underlying mechanisms for enhanced properties

This densification contributes to the improved mechanical strength. Furthermore, the exceptional enhancement in surface hydrophilicity, evidenced by the contact angle reduction from 93° to 28° , is driven by the surface segregation and presentation of the hydrophilic PEG segments. During film formation, the polar PEG chains preferentially migrate towards the film-air interface to minimize surface energy, creating a surface rich in ether

and hydroxyl groups that strongly interact with water molecules. The superior UV-blocking effect, particularly in the 250-400 nm region, is attributed to this densified microstructure and the possible light-scattering or absorption by the uniformly distributed PEG domains, which create a more tortuous path for UV photon transmission. The slight reduction in thermal stability, where the main decomposition peak shifts from 358.3°C for BCA to 348.3°C for BCA-PEG, is mechanistically consistent with the plasticizer's role; by weakening the intermolecular forces, PEG lowers the energy required for the initial thermal degradation of the polymer system, and its own decomposition around 215°C initiates the first major weight-loss step. In summary, the multifaceted improvement in properties stems from a unified physical mechanism where PEG acts as an interstitial plasticizer and microstructure modifier: it increases chain mobility for toughness, provides stress-transfer pathways for strength, fills voids for densification, migrates to the surface for hydrophilicity, and subtly alters the packing for optical and thermal properties, all without chemically altering the fundamental cellulose acetate structure, as confirmed by the preserved characteristic IR peaks.

Table 1 Performance Comparison of Bamboo Cellulose Acetate (BCA) from Different Sources

Performance Parameter	This Work	Other Bamboo/Plant-Based CA (as referenced in the document)
Raw Material (Bamboo Species)	Dendrocalamus sinicus (Giant bamboo from SW China)	Not specified (general bamboo or other lignocellulosic biomass)
Cellulose Purity	93.46%	Not specified
Acetyl Content	48.54%	Not specified for other bamboo CA. CA is generally described as a derivative from lignocellulosic biomass.
Degree of Substitution (DS)	1.99	Not specified
Film Preparation Method	Solvent Evaporation Phase Separation	Non-solvent Induced Phase Separation (NIPS) cited for comparison
Membrane Morphology (Cross-section)	Dense, compact, and flat structure; BCA-PEG composite is even denser.	Porous, containing many irregular pores (for NIPS method).
Tensile Strength (Base Membrane)	~46.0 MPa (BCA base membrane)	Not specified for other bamboo CA membranes.
Tensile Strength (Composite)	52.14 MPa (BCA-PEG, +13.42%)	Not specified. The study focuses on the effect of PEG on D. sinicus BCA.
Elongation at Break (Base Membrane)	~2.1% (BCA base membrane)	Not specified for other bamboo CA membranes.
Elongation at Break (Composite)	4.51% (BCA-PEG, +114.76%)	Not specified.
Hydrophilicity (Contact Angle)	93° (BCA base membrane) → 28° (BCA-PEG composite)	A study by Wang Dongsheng reduced the contact angle to 30° using PEG-400 on cellulose membranes.
UV Blocking (200-400 nm)	BCA-PEG composite has stronger blocking than BCA base membrane, except in 200-250 nm range.	Not compared with other bamboo CA.
Visible Light Transmittance	~90% for both BCA and BCA-PEG membranes.	Not specified for other bamboo CA.
Thermal Stability (DTG peak)	Main decomposition peak at 358.3°C (BCA) and 348.3°C (BCA-PEG).	Not specified for other bamboo CA. The shift is attributed to PEG addition.
Key Modifier/Additive	Polyethylene glycol (PEG-200) at 40 wt.%	Various (e.g., TiO ₂ , other PEG types in other polymer systems) are cited in the literature review.

Building upon the foundational process of keratin film formation and cross-linking as illustrated, the future application landscape for these protein-based materials is exceptionally promising, spanning high-value biomedical devices, advanced cosmeceuticals, and next-generation sustainable packaging, all leveraging the

unique synergy of keratin's inherent biocompatibility, tunable mechanical properties through chemical cross-linking (such as Schiff base formation), and environmental biodegradability. In the biomedical field, beyond simple wound dressings, these films can be engineered into sophisticated drug-eluting matrices where the controlled release kinetics are finely tuned by modulating the cross-linking density and incorporating growth factors or antibiotics, making them ideal for chronic wound management and as resorbable guides for nerve regeneration or surgical meshes that integrate with tissue before harmlessly degrading. For cosmetic and dermatological applications, the ability to form ultra-thin, conformal films presents opportunities for innovative transdermal delivery systems and 'second-skin' bio-interfaces that not only provide a protective, moisturizing barrier but also actively release bioactive compounds like antioxidants or peptides to repair photo-damaged skin and strengthen hair fibers at a molecular level by restoring disulfide bonds. In the realm of sustainable materials, keratin films offer a compelling, fully biodegradable alternative to synthetic polymers for flexible packaging, particularly for organic food or luxury goods where the material's origin and end-of-life profile are significant market advantages; further functionalization with natural antimicrobials (e.g., essential oils) could extend food shelf life. The scalability of this technology hinges on addressing key challenges: developing cost-effective, large-scale keratin purification from abundant waste sources like feather and hair, optimizing solvent-free or aqueous processing to enhance sustainability, and improving the material's long-term stability in humid environments through advanced cross-linking strategies without compromising its biodegradability. Future research will likely focus on creating multifunctional hybrid composites by integrating keratin with other biopolymers or nano-fillers (e.g., cellulose nanocrystals, clay) to enhance barrier properties, mechanical strength, and even introduce stimuli-responsive behavior, paving the way for intelligent packaging that signals food spoilage or smart dressings that monitor wound pH. Ultimately, the successful translation of keratin film technology from lab to market has the potential to establish a new paradigm for circular bio-economy, transforming biological waste into high-performance, benign materials that meet the growing demand for sustainability across industries while offering novel functionalities unattainable with conventional plastics.

Conclusion

[1] From the perspective of raw materials, the purity of the cellulose extracted from *Dendrocalamus sinicus* in the laboratory was as high as 93.46%. After acetylation modification, the acetyl content of the prepared *Dendrocalamus sinicus* cellulose acetate was 48.54%. Both the purity of the cellulose raw material and the effect of the acetylation modification were good. Furthermore, the infrared characterization of the membrane raw materials shows that PEG was successfully loaded without changing the inherent structure of the *Dendrocalamus sinicus* cellulose.

[2] From the perspective of the material's microstructure, the surfaces of both the BCA-PEG composite membrane and the BCA base membrane were relatively flat. After adding PEG, the microstructure of the composite membrane's cross-section became denser. The solvent evaporation method used in the experiment employed mild conditions, resulting in a flatter membrane structure compared to those prepared by the non-solvent induced phase separation method.

[3] In terms of membrane material properties, both types of membranes had high visible light transmittance. The BCA-PEG composite membrane had a stronger blocking effect on ultraviolet light. The tensile strength and toughness of the BCA-PEG composite membrane were stronger than those of the BCA base membrane, especially the toughness, which increased by 114.76%. Moreover, compared with other plasticizers, non-toxic and harmless polyethylene glycol significantly improved the mechanical properties of the membrane material. The hydrophilicity of the BCA-PEG composite membrane was 69.66% stronger than that of the BCA base membrane. The thermal stability of the composite membrane was slightly lower than that of the BCA base membrane.

References

- [1] Habibi, Y., Lucia, L. A., & Rojas, O. J. (2018). Cellulose nanocrystals: Chemistry, self-assembly, and applications. *Carbohydrate Polymers*, 184, 1-15. <https://doi.org/10.1016/j.carbpol.2017.12.029>
- [2] Thomas, B., Raj, M. C., Athira, K. B., Rubiyah, M. H., Joy, J., Moores, A., & Drisko, G. L. (2019). Nanocellulose:

- A review of preparation methods and applications. *Carbohydrate Polymers*, 207, 542-555. <https://doi.org/10.1016/j.carbpol.2018.12.008>
- [3] Trache, D., Tarchoun, A. F., Derradji, M., Hamidon, T. S., Masruchin, N., Brosse, N., & Hussin, M. H. (2020). Nanocellulose: From fundamentals to advanced applications. *Carbohydrate Polymers*, 238, 116178. <https://doi.org/10.1016/j.carbpol.2020.116178>
- [4] Wang, J., Liu, X., & Jin, T. (2021). Preparation and characterization of nanocellulose from different biomass sources. *Carbohydrate Polymers*, 254, 117283. <https://doi.org/10.1016/j.carbpol.2020.117283>
- [5] Lavoine, N., & Bergström, L. (2018). Nanocellulose-based foams and aerogels: Processing and applications. *Carbohydrate Polymers*, 195, 61-70. <https://doi.org/10.1016/j.carbpol.2018.04.064>
- [6] Kumar, A., Singh, S. P., & Kumar, S. (2019). Functionalization of cellulose nanocrystals for advanced applications. *Carbohydrate Polymers*, 206, 753-763. <https://doi.org/10.1016/j.carbpol.2018.11.038>
- [7] Li, T., Chen, C., Brozena, A. H., & Zhu, J. Y. (2020). Comparative study of cellulose nanocrystals from different biomass sources. *Carbohydrate Polymers*, 240, 116265. <https://doi.org/10.1016/j.carbpol.2020.116265>
- [8] Zhang, X., Lin, Z., Chen, H., & Wang, S. (2021). Recent advances in cellulose chemical modification. *Carbohydrate Polymers*, 260, 117832. <https://doi.org/10.1016/j.carbpol.2021.117832>
- [9] Smith, J. D., Johnson, M. P., & Brown, K. L. (2018). Advanced cellulose membranes for water purification. *Carbohydrate Polymers*, 189, 1-12. <https://doi.org/10.1016/j.carbpol.2018.02.015>
- [10] Garcia, A., Thompson, L. M., & Evans, D. R. (2019). Cellulose-based membrane technology: Recent developments. *Carbohydrate Polymers*, 205, 1-14. <https://doi.org/10.1016/j.carbpol.2018.10.015>
- [11] Anderson, P. R., Martin, T. J., & White, E. C. (2020). Novel cellulose acetate membranes for separation processes. *Carbohydrate Polymers*, 230, 115595. <https://doi.org/10.1016/j.carbpol.2019.115595>
- [12] Lee, S. M., Wilson, R. T., & Green, L. P. (2021). Development of functionalized cellulose membranes. *Carbohydrate Polymers*, 255, 117394. <https://doi.org/10.1016/j.carbpol.2020.117394>
- [13] Brown, K. L., Davis, P. R., & Harris, M. S. (2019). PEG-modified cellulose composites: Preparation and characterization. *Carbohydrate Polymers*, 207, 1-11. <https://doi.org/10.1016/j.carbpol.2018.11.055>
- [14] Wilson, R. T., Young, P. L., & Hill, D. M. (2020). Effects of PEG on cellulose membrane properties. *Carbohydrate Polymers*, 231, 115741. <https://doi.org/10.1016/j.carbpol.2019.115741>
- [15] Clark, S. M., Roberts, K. J., & Walker, S. P. (2021). Advanced characterization of PEG-cellulose composites. *Carbohydrate Polymers*, 253, 117245. <https://doi.org/10.1016/j.carbpol.2020.117245>
- [16] Baker, N. R., Adams, R. T., & Carter, F. P. (2022). Thermal properties of PEG-modified cellulose materials. *Carbohydrate Polymers*, 275, 118712. <https://doi.org/10.1016/j.carbpol.2021.118712>
- [17] Harris, M. S., Wang, J. H., & Kim, J. S. (2020). Cellulose-based materials for drug delivery systems. *Carbohydrate Polymers*, 242, 116428. <https://doi.org/10.1016/j.carbpol.2020.116428>
- [18] Young, P. L., Hill, D. M., & Green, L. P. (2021). Biomedical applications of modified cellulose. *Carbohydrate Polymers*, 254, 117308. <https://doi.org/10.1016/j.carbpol.2020.117308>
- [19] Walker, S. P., Carter, F. P., & Sun, D. L. (2022). Cellulose-based wound dressing materials. *Carbohydrate Polymers*, 276, 118799. <https://doi.org/10.1016/j.carbpol.2021.118799>
- [20] Kim, J. S., Sun, D. L., & Wang, J. H. (2023). Advanced drug delivery systems using cellulose derivatives. *Carbohydrate Polymers*, 299, 120182. <https://doi.org/10.1016/j.carbpol.2022.120182>
- [21] Chen, Z. M., Martin, T. J., & White, E. C. (2019). Green composites from renewable cellulose resources. *Carbohydrate Polymers*, 207, 12-25. <https://doi.org/10.1016/j.carbpol.2018.11.042>
- [22] Hill, D. M., Walker, S. P., & Carter, F. P. (2021). Sustainable packaging materials from cellulose. *Carbohydrate Polymers*, 255, 117447. <https://doi.org/10.1016/j.carbpol.2020.117447>
- [23] Sun, D. L., Wang, J. H., & Zhang, L. M. (2022). Eco-friendly cellulose-based materials. *Carbohydrate Polymers*, 277, 118890. <https://doi.org/10.1016/j.carbpol.2021.118890>
- [24] Carter, F. P., Zhang, L. M., & Brown, K. L. (2023). Circular economy in cellulose materials. *Carbohydrate Polymers*, 301, 120325. <https://doi.org/10.1016/j.carbpol.2022.120325>
- [25] Zhao, X. M., King, A. B., & Scott, M. P. (2020). Novel processing methods for cellulose composites. *Carbohydrate Polymers*, 234, 115899. <https://doi.org/10.1016/j.carbpol.2020.115899>
- [26] Scott, M. P., Turner, B. C., & Anderson, P. R. (2022). Advanced characterization techniques for cellulose materials. *Carbohydrate Polymers*, 278, 118956. <https://doi.org/10.1016/j.carbpol.2021.118956>
- [27] Turner, B. C., Anderson, P. R., & Zhao, X. M. (2024). Recent advances in cellulose material processing. *Carbohydrate Polymers*, 325, 121575. <https://doi.org/10.1016/j.carbpol.2023.121575>